Deep and bottom water export from the Southern Ocean to the Pacific over the past 38 million years

Tina van de Flierdt,[1,2] Martin Frank,[1] Alex N. Halliday,[1] James R. Hein,[3] Bodo Hattendorf,[4] Detlef Günther,[4] and Peter W. Kubik[5]

Received 10 May 2003; revised 6 November 2003; accepted 23 January 2004; published 10 March 2004.

[1] The application of radiogenic isotopes to the study of Cenozoic circulation patterns in the South Pacific Ocean has been hampered by the fact that records from only equatorial Pacific deep water have been available. We present new Pb and Nd isotope time series for two ferromanganese crusts that grew from equatorial Pacific bottom water (D137-01, "Nova," 7219 m water depth) and southwest Pacific deep water (63KD, "Tasman," 1700 m water depth). The crusts were dated using $^{10}Be/^{9}Be$ ratios combined with constant Co-flux dating and yield time series for the past 38 and 23 Myr, respectively. The surface Nd and Pb isotope distributions are consistent with the present-day circulation pattern, and therefore the new records are considered suitable to reconstruct Eocene through Miocene paleoceanography for the South Pacific. The isotope time series of crusts Nova and Tasman suggest that equatorial Pacific deep water and waters from the Southern Ocean supplied the dissolved trace metals to both sites over the past 38 Myr. Changes in the isotopic composition of crust Nova are interpreted to reflect development of the Antarctic Circumpolar Current and changes in Pacific deep water circulation caused by the build up of the East Antarctic Ice Sheet. The Nd isotopic composition of the shallower water site in the southwest Pacific appears to have been more sensitive to circulation changes resulting from closure of the Indonesian seaway. *INDEX TERMS:* 4267 Oceanography: General: Paleoceanography; 4808 Oceanography: Biological and Chemical: Chemical tracers; 9355 Information Related to Geographic Region: Pacific Ocean; *KEYWORDS:* Pacific Ocean, deep water circulation, radiogenic isotopes

Citation: van de Flierdt, T., M. Frank, A. N. Halliday, J. R. Hein, B. Hattendorf, D. Günther, and P. W. Kubik (2004), Deep and bottom water export from the Southern Ocean to the Pacific over the past 38 million years, *Paleoceanography*, *19*, PA1020, doi:10.1029/2003PA000923.

1. Introduction

[2] Global ocean circulation has been strongly influenced by major changes in paleogeography during the Cenozoic. For example, plate-tectonic movements opened and closed oceanic seaways, which led to large-scale reorganization of interocean pathways and hence changed deep water mass exchange, heat and salinity budgets, and ultimately global climate (for a recent summary, see *Zachos et al.* [2001]).

[3] The Southern Ocean plays a crucial role in the present-day global ocean current system ("global conveyor belt" model; *Broecker* [1991]). The connection between all three major ocean basins provided by the Antarctic Circumpolar Current (ACC) not only permits efficient global water mass exchange, but also dominates transport of heat, fresh water, and other properties that influence climate [e.g., *Rintoul et al.*, 2001; *Schmitz*, 1995]. The ACC is a geostrophic eastward flow that extends from the surface to the deep ocean and represents the largest present-day ocean current in terms of volume transport. Several sites of Antarctic Bottom Water (AABW) formation occur within the Southern Ocean, the most important of which is the Weddell Sea (see *Rintoul et al.* [2001] for a recent summary). AABW, however, is not circumpolar because it is too dense to flow over the sill of Drake Passage [*Orsi et al.*, 1999]. The water mass circulating with the ACC is the Circumpolar Deep Water (CDW) and is predominantly a mixture of AABW and North Atlantic Deep Water (NADW) [*Schmitz*, 1996]. Modified AABW and CDW are exported from the ACC to the Atlantic, Pacific and Indian Oceans.

[4] In the past, circulation of water around Antarctica was prevented by the connection of Australia to Antarctica (Tasmanian gateway: opened ~33 Ma) and South America to Antarctica (Drake Passage: opened between ~30 and ~20 Ma). At the same time, open gateways in the Indonesian area (Indonesian gateway), between North and South America (Isthmus of Panama), and interoceanic gateways between the Tethys and Atlantic and Indian Oceans (at least in Eocene times; *Oberhänsli* [1992]) allowed equatorial interbasin water mass exchange. However, it is not clear where deep water formation took place in Eocene through Miocene times and what the deep water circulation pattern

[1]Institute for Isotope Geology and Mineral Resources, Department of Earth Sciences, Eidgenossische Technische Hochschule, Zürich, Switzerland.
[2]Now at Lamont-Doherty Earth Observatory, Columbia University, Palisades, New York, USA.
[3]U.S. Geological Survey, Menlo Park, California, USA.
[4]Laboratory of Inorganic Chemistry, Department of Chemistry, Eidgenossische Technische Hochschule, Zürich, Switzerland.
[5]Paul Scherrer Institute, c/o Institute for Particle Physics, Eidgenossische Technische Hochschule, Zürich, Switzerland.

0883-8305/04/2003PA000923

looked like. Since polar regions were much warmer in the early Eocene than today (see *Zachos et al.* [2001] and *Lear et al.* [2000] for recent summaries), salty water from middle and low latitudes was probably densest, resulting in warm deep waters at the time. Hypotheses about Eocene through Miocene deep water circulation have been summarized by several authors [e.g., *Kennett and Stott*, 1990; *Wright et al.*, 1992; *Wright and Miller*, 1993; *Flower and Kennett*, 1995; *Ramsay et al.*, 1998]. By the late middle Miocene, deep water circulation patterns similar to those of today were established. The early Eocene through late middle Miocene Earth experienced a transition from warm polar climates in the early Eocene to a global climate and deep water circulation pattern similar to the present [e.g., *Wright and Miller*, 1993]. One of the most important variables was the extent of ice accumulation on Antarctica. At about 15 Ma, the major East Antarctic Ice Shield (EAIS) became a permanent feature, coincident with a significant deep ocean cooling [see *Billups and Schrag*, 2002; *Flower and Kennett*, 1995, and references therein] and increased production and export of deep water from the Southern Ocean.

[5] Most of the above conclusions about Cenozoic climate and ocean circulation are based on $\delta^{18}O$ and $\delta^{13}C$ records from ODP and DSDP drilling sites. While oxygen isotopes give valuable information about deep ocean temperature and continental ice volume, carbon isotopes are the most commonly applied geochemical proxy to reconstruct past deep water circulation. For $\delta^{13}C$, however, nonconservative effects of temperature, nutrient availability (see overview by *Broecker and Peng* [1982]), and carbonate ion concentration [*Spero et al.*, 1997] complicate the record. Moreover, $\delta^{13}C$ is essentially a tracer of nutrient concentration, which is controlled by processes in the surface ocean. Thus deep water masses of different origins within an ocean basin may not be distinguishable by the $\delta^{13}C$ signatures [*Frank*, 2002]. Several studies using radiogenic isotope time series (e.g., Pb, Nd) obtained from ferromanganese crusts have provided valuable information about the effects of climatic and paleogeographic variations on deep water composition and circulation patterns (for a recent summary, see *Frank* [2002]).

[6] Neodymium has an average ocean residence time of between 600 and 2000 years [*Jeandel*, 1993; *Jeandel et al.*, 1995; *Tachikawa et al.*, 1999], which is long enough to be dispersed within the global thermohaline circulation system and short enough to avoid homogenization. Consequently, the Nd isotope system has been considered a suitable radiogenic isotope tracer to monitor large-scale changes in ocean circulation. The Nd isotopic composition of a particular deep water mass is essentially dependent on two factors: (1) the erosional load delivered to the oceans from the continents and (2) variation of these source signatures through vertical and lateral mixing with other water masses.

[7] In contrast, the residence time of Pb in deep water is short (~50 to 200 years; *Craig et al.* [1973], *Schaule and Patterson* [1981], *Cochran et al.* [1990]). Consequently, dissolved Pb isotopes in the oceans are influenced by local sources such as riverine inputs, eolian dust accumulation, and hydrothermal activity [e.g., *Frank et al.*, 1999b; *Vlastélic et al.*, 2001]. Recent studies suggest, however, that Pb isotopes can be advected over quite long distances and can be suitable tracers for water mass movement and mixing within ocean basins [*Abouchami and Goldstein*, 1995; *Abouchami et al.*, 1997; *von Blanckenburg and Igel*, 1999; *Claude-Ivanaj et al.*, 2001; *van de Flierdt et al.*, 2003].

[8] This study focuses on the radiogenic isotope history of the deep South Pacific, which is a key area for the understanding of the development of the global deep water circulation. We present new combined isotope time series (Pb, Nd) obtained from ferromanganese crusts from the southwest Pacific and southern equatorial Pacific. These two locations monitored the evolution of inflowing deep water masses from the Southern Ocean and water mass mixing within the Pacific Ocean and therefore provide new constraints on the Eocene through Miocene deep water circulation patterns in the South Pacific.

2. Samples, Locations, and Background

[9] Two ferromanganese crusts, one that grew from equatorial Pacific bottom water and one from southwest Pacific deep water (Figure 1), were selected to investigate the evolution of inflowing deep and bottom water masses from the Southern Ocean. A third crust from the deep equatorial Pacific was studied to confirm the end-member isotopic composition of equatorial Pacific deep water.

2.1. Equatorial Pacific Bottom Water-Crust Nova

[10] Crust D137-01 (01°08.0S, 168°04.0′W; 117.5 mm thick), hereafter called "Nova," was dredged during cruise Nova IX (1979) in the Nova Canton Trough from a water depth of 7129 m. The massive crust grew on a hyaloclastite substrate and displays macroscopically visible growth banding. It is the deepest water ferromanganese crust analyzed so far and it recorded changes in equatorial Pacific bottom water, the composition of which ultimately reflects modified AABW. Today, the main export pathway of deep water from the ACC to the Pacific is the Deep Western Boundary Current (DWBC). This current separates from the ACC east of the Campbell Plateau at 49 °S and flows northward along the continental rise east of New Zealand and along the Tonga-Kermadec Ridge (e.g., *Carter and Wilkin* [1999]; Figure 1). *Wijffels et al.* [2001] and *Reid* [1997] suggested that above and somewhat offset to the east of this world's largest DWBC, a significant amount of Pacific Deep Water (PDW) flows southward and hence is exported out of the Pacific Ocean. Further north at 10°S (169–170°E) the deep and abyssal waters of the DWBC travel through a ~200 km wide and 3500–5200 m deep passage, the Samoan Passage, which is the only major conduit for abyssal waters moving northward [*Reid and Lonsdale*, 1974; *Taft et al.*, 1991; *Johnson et al.*, 1994; *Rudnick*, 1997]. The Nova Canton Trough is situated exactly north of the exit of the Samoan Passage (Figure 1). The deepest part of the trough (> 4000 m) has most likely been filled with modified AABW transported northward as part of the DWBC.

2.2. Southwest Pacific Deep Water-Crust Tasman

[11] Crust 63KD (28°34.0S, 163°00.0′E; 39 mm thick), hereafter called "Tasman," was recovered on Lord Howe Rise during the SO36 cruise (Figure 1) from a water depth

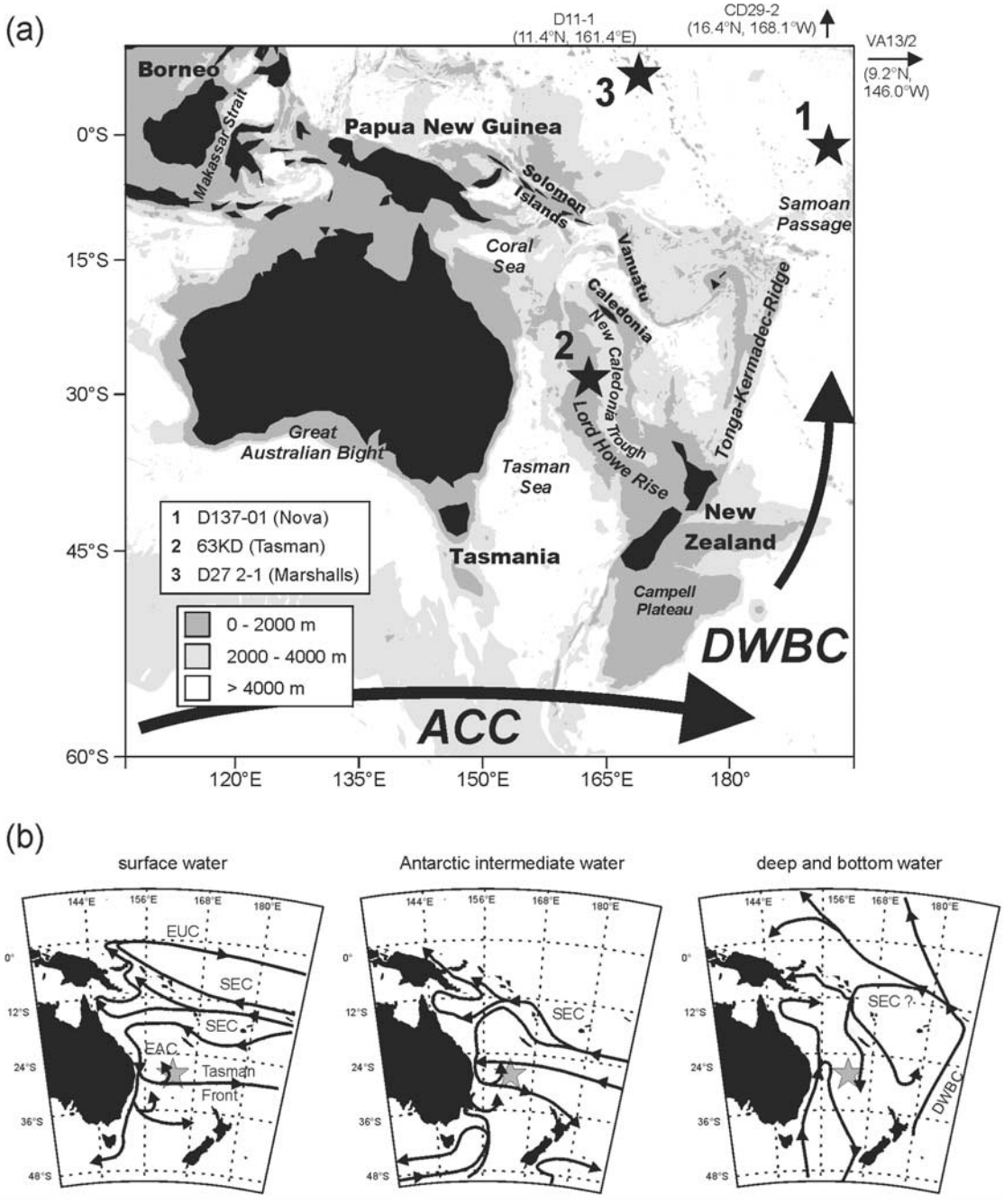

Figure 1. (a) Sample locations, bathymetry, and area names in the South Pacific. Black arrows indicate very schematically the two main currents of the region. Abbreviations are as follows: ACC, Antarctic Circumpolar Current; DWBC, Deep Western Boundary Current. (b) Blow up of the southwest Pacific showing the surface, intermediate, and deep/bottom water circulation as taken from *Sokolov and Rintoul* [2000]. The gray star is the location of crust Tasman. Abbreviations are as follows: EUC, Equatorial Undercurrent; SEC, South Equatorial Current; EAC, East Australian Current.

of 1700 m. This dense crust shows partly bent, thin laminations, subparallel to the growth surface. The distance of the crust site to Australia is about 900 km and the northern tip of New Zealand is about 1100 km away. The entire region east of Australia and west of New Zealand and the Tonga-Kermadec ridge is made up of a number of individual basins with differing depths and extents. This leads to complex pathways for present-day circulation as outlined in Figure 1 for surface, intermediate, and deep and bottom water [*Sokolov and Rintoul*, 2000]. The primary inflowing surface water mass into the region is the westward flowing South Equatorial Current (SEC) (*Wyrtki*

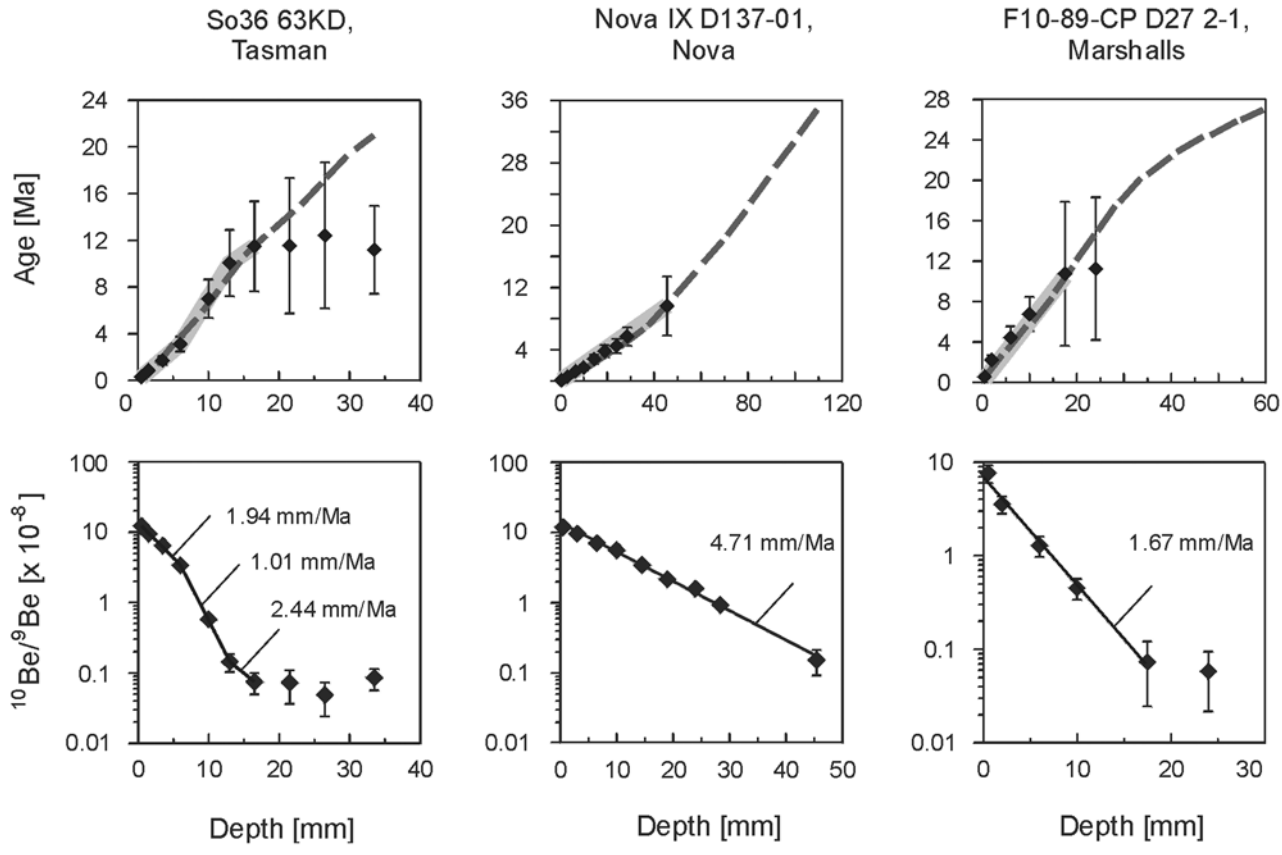

Figure 2. Calculated age and $^{10}Be/^{9}Be$ versus depth for crusts Tasman, Nova, and Marshalls. Ages have been calculated with a half-life for ^{10}Be of 1.5 Myr and assuming a constant initial $^{10}Be/^{9}Be$ ratio. Solid lines represent the Be-derived age model, with corresponding growth rates. The dashed lines show the age model calculated using the Co growth rate relationship [*Manheim*, 1986], which was calibrated to match the $^{10}Be/^{9}Be$ dating of the younger parts.

[1960]; Figure 1). Important for understanding the setting of crust Tasman is the fact that the SEC has an extension at depth that includes Antarctic Intermediate Water (AAIW) and deep and bottom waters (*Sokolov and Rintoul* [2000]; Figure 1). Lord Howe Rise acts as a barrier for deep and bottom water in the southwest Pacific, which separates into western and eastern branches (Figure 1). The western area is the Tasman Sea and represents the only basin where a northward flow of deep and bottom water with Southern Ocean characteristic has been identified [*Sokolov and Rintoul*, 2000]. The Tasman Sea is, however, closed to the north below 2800 m [*Wijffels et al.*, 2001]. Moreover, Lord Howe Rise inhibits an inflow of Southern Ocean water to the eastern basins. Therefore all eastern basins receive deep and bottom waters from the equatorial Pacific, most likely delivered by the SEC [*Wijffels et al.*, 2001] (Figure 1). This also applies to crust Tasman, which was recovered from the eastern flank of Lord Howe Rise.

2.3. Equatorial Pacific Deep Water-Crust Marshalls

[12] During cruise F10-89-CP, crust D27 2-1 (hereafter called "Marshalls") was dredged from a seamount in the Marshall Islands area of the western equatorial Pacific (07°31′N, 169°40′E, 1670–1570 m water depth). This 68 mm thick, massive crust grew from Pacific deep water. Since location and water depth are similar to previously investigated crusts D11-1 and CD29-2 (*Ling et al.* [1997]; Figure 1), crust Marshalls is only taken as representative of the predefined equatorial Pacific deep water end-member and will not be subject to discussion beyond that.

3. Methods

[13] Aliquots of manually sampled depth profiles of the three crusts were used to determine concentrations of ^{10}Be, ^{9}Be, and major and trace elements (Fe, Mn, Co, Ni, Cu). Sampling for Pb and Nd isotope profiles was carried out using a computer-controlled milling device to obtain continuous high-resolution time series.

[14] Age models for all three crusts are based on $^{10}Be/^{9}Be$ ratios (Figure 2; Tables 1 and 2). Chemical preparation of 5 to 10 mg sample material for the AMS measurements of ^{10}Be concentrations closely followed a previously described method [*Henken-Mellies et al.*, 1990]. The ^{10}Be concentrations were measured at the Zürich AMS facility of the Paul Scherrer Institute and ETH Zürich, Switzerland. In order to cancel out dilution effects, all ^{10}Be data were normalized to stable ^{9}Be, which was measured on the same

Table 1. Be and Co Concentrations for Crusts Tasman, Nova, and Marshalls[a]

Depth Interval, mm	^{10}Be [atoms/g]*10^{-8}, ±1σ S.E.	^{9}Be$_{measured}$, ppm	^{9}Be$_{corr}$, ppm	^{10}Be/^{9}Be *10^{-8}, ±1s S.E.	Co$_{measured}$, ppm	Co$_{corr}$, ppm
			So36 63KD (Tasman)			
0–1.0	546 ± 5.50	1.0	1.7	12.15 ± 2.48	879.4	1398
1–2	351.9 ± 13.1	3.2	5.6	9.39 ± 1.91	2297	3652
3–4	209.7 ± 14.4	2.8	4.9	6.36 ± 1.35	2335	3713
5.5–6.5	92.9 ± 4.9	2.4	4.2	3.34 ± 0.69	2177	3462
9.5–10.5	25.25 ± 3.08	3.8	6.7	0.57 ± 0.13	2380	3785
12.5–13.5	7.90 ± 1.58	4.7	8.4	0.14 ± 0.04	2534	4029
16–17	4.08 ± 1.10	4.7	8.3	0.07 ± 0.02	1897	3016
21–22	1.81 ± 3.93	4.6	8.2	0.07 ± 0.04	1962	3120
26–27	1.20 ± 2.61	4.6	8.2	0.05 ± 0.02	2154	3424
33–34	1.19 ± 4.39	4.4	7.8	0.08 ± 0.03	1681	2673
			Nova IX D137-01 (Nova)			
0–1.0	243.7 ± 10.08	1.7	3.1	11.88 ± 2.43	884.5	1406
2.5–3.5	319.4 ± 15.11	2.8	4.9	9.67 ± 1.99	1308	2080
6–7	243.0 ± 11.52	2.9	5.2	7.05 ± 1.45	1260	2004
9.5–10.5	215.6 ± 7.18	3.3	5.8	5.61 ± 1.14	1361	2164
14–15	130.3 ± 4.53	3.2	5.7	3.44 ± 0.12	1441	2291
18.5–19.5	94.7 ± 3.97	3.7	6.6	2.16 ± 0.44	1457	2316
23.5–24.5	68.96 ± 2.95	3.7	6.5	1.59 ± 0.33	1555	2472
28–29	42.79 ± 1.99	4.0	7.0	0.91 ± 0.19	1515	2409
45–46	7.37 ± 2.50	4.1	7.2	0.15 ± 0.06	1956	3110
63–64	< blank	3.4	6.0		2124	3377
84.5–85.5	< blank	4.1	7.3		2334	3711
109–110	< blank	4.7	8.4		2285	3633
			F10-89-CP D27 2-1 (Marshalls)			
0–1.0	134.1 ± 9.84	1.5	2.6	7.62 ± 1.62	4423	7033
1.5–2.5	102.2 ± 6.00	2.4	4.3	3.55 ± 0.74	4638	7374
5.5–6.5	54.09 ± 7.57	3.6	6.3	1.28 ± 0.31	4465	7100
9.5–10.5	18.24 ± 2.76	3.4	6.1	0.45 ± 0.01	4078	6484
17–18	3.60 ± 2.28	4.2	7.4	0.07 ± 0.05	5417	8613
23.5–24.5	3.40 ± 2.02	5.0	8.8	0.06 ± 0.04	4558	7247
29–30	< blank	3.7	6.5		4228	6722
35–36	< blank	2.2	3.9		3395	5397
47–48	< blank	2.2	3.9		2601	4136
58.5–59.5	< blank	3.3	5.8		2385	3792

[a]Measured Be and Co concentration data correspond to the original ICP-MS analysis. The corrected data are normalized to the ratio between the measured values in Nod A-1 and the values published by *Axelsson et al.* [2002]. For further explanations, see section 3 and *van de Flierdt et al.* [2003].

aliquots at the Laboratory of Inorganic Chemistry, ETH Zürich, Switzerland, using an ELAN DRC ICP-MS 6100 instrument. Further details about both methods can be found in the work of *van de Flierdt et al.* [2003].

[15] For Pb isotope analysis, 1 mg of sample powder was first leached for 15 min on a warm hotplate with 6M HCl and any undissolved material (detrital) was separated from the solution by centrifugation. Following this initial step, the chemical separation closely followed that described by *Lugmair and Galer* [1992]. The Pb isotope ratios were measured with a Nu Plasma MC-ICP-MS at the ETH Zürich using a Tl-doping procedure to correct for instrumental mass bias [*Walder et al.*, 1993]. Repeat analyses of the NIST SRM981 Pb standard during the measurements of the individual three crusts gave the external reproducibility (2 σ standard deviation) reported in Table 3[1]. The long-term reproducibility, however, based on several ferromanganese crust measurement sessions over 3 years (Nu Plasma MC-ICP-MS, ETH Zürich), indicates a slightly worse external precision (2 σ standard deviation) of 100–130 ppm for ^{206}Pb/^{204}Pb, 100–160 ppm for ^{207}Pb/^{204}Pb, and 100–200 ppm for ^{208}Pb/^{204}Pb. All reported Pb isotope results were normalized to the Pb isotopic composition of NIST SRM981 given by *Galer and Abouchami* [1998].

[16] Neodymium chemistry using ∼10 mg samples was carried out following the separation and purification method described by *Cohen et al.* [1988]. Neodymium measurements were performed by MC-ICP-MS. To correct for instrumental mass bias ^{143}Nd/^{144}Nd ratios were normalized to ^{146}Nd/^{144}Nd of 0.7219. Repeated analysis of the JMC Nd standard yielded 0.511813 ± 10 (2 σ standard deviation, n = 24) and 0.511804 ± 15 (n = 17) during the two measuring sessions of crusts Tasman and Nova, respectively. To compare our JMC values with the commonly used La Jolla standard, several cross calibrations were carried out that gave a constant difference in ^{143}Nd/^{144}Nd of 0.000025 between the two standard solutions. ^{143}Nd/^{144}Nd ratios are reported relative to a JMC value of 0.511833, which is equivalent to a nominal La Jolla value of 0.511858. The precision of duplicate sample measurements on different days (same solutions) and of repeat samples run independently through the chemistry was within the external reproducibility of the

[1]Auxiliary Table 3 is available electronically at the PANGAEA Database, Alfred-Wegener-Instit. für Polar- und Meeresforsch., Columbusstrasse, D-27568 Bremerhaven, Germany (info@pangaea.de; URL: http://www.pangaea.de).

Table 2. Growth Rates for Crusts Tasman, Nova, and Marshalls

So36 63 KD (Tasman)		NovaIX D137-01 (Nova)		F10-89-CP D27 2-1 (Marshalls)	
Depth Interval, mm	Growth Rate, mm/Ma	Depth Interval, mm	Growth Rate, mm/Ma	Depth Interval, mm	Growth Rate, mm/Ma
0–6	1.94[a]	0–45.5	4.71[a]	0–17.5	1.67[a]
6–13	1.01[a]	45.5–54.5	3.12[b]	17.5–20.75	1.26[b]
13–16.5	2.44[a]	54.5–74.25	2.72[b]	20.75–26.75	1.69[b]
16.5–19	1.90[b]	74.25–97.25	2.32[b]	26.75–32.5	1.91[b]
19–24	1.80[b]	97.25–bottom	2.41[b]	32.5–41.5	2.76[b]
24–30	1.54[b]			41.5–53.25	4.31[b]
30-bottom	2.33[b]			53.25-bottom	4.99[b]

[a]Derived from $^{10}Be/^{9}Be$ data.
[b]Derived from constant Co flux model.

standard measurements (Table 3[2]). All Pb and Nd isotope data are available on request from the corresponding author or electronically via the PANGAEA database.

4. Results

[17] Major and trace element compositions for all three crusts show concentrations typical of hydrogenous growth and X-ray diffraction analysis showed no evidence of phosphatization in crusts Marshalls and Nova. This is important, because there has been an ongoing debate about whether phosphatization is able to alter the isotopic composition in the older parts of time series records [*Ling et al.*, 1997; *Christensen et al.*, 1997; *Frank et al.*, 1999a].

4.1. Crust Chronologies and Growth Rates

[18] ^{10}Be, ^{9}Be, Co concentrations, $^{10}Be/^{9}Be$ ratios, and calculated growth rates for all three crusts are presented in Tables 1 and 2. $^{10}Be/^{9}Be$ ratios are plotted as a function of depth in the crusts with two different calculated age-depth relationships (Figure 2): (1) based on the best fit of the $^{10}Be/^{9}Be$ data and (2) applying a constant Co-flux model [*Manheim*, 1986; *Frank et al.*, 1999a]. The constant Co-flux model was tuned to fit the $^{10}Be/^{9}Be$-derived growth rates in the younger parts of the crusts. The results of the two models are shown in Figure 2 together with individual ages calculated for each measured $^{10}Be/^{9}Be$ ratio. Assuming a constant initial $^{10}Be/^{9}Be$ ratio for crust Nova, all 9 measured $^{10}Be/^{9}Be$ ratios define an exponential curve that implies a constant growth rate of 4.7 mm/Ma for the uppermost 45.5 mm of the crust, in good agreement with near constant Co concentrations (Table 1). No ^{10}Be was detected below the depth of 45.5 mm. The constant Co-flux model was applied and resulted in slightly lower growth rates (Table 2). For crust Tasman, a constant growth rate is not within error of all $^{10}Be/^{9}Be$ data. The growth rates that give the best exponential fit vary between 1.0 and 2.4 mm/Ma for the uppermost 16.5 mm (Figure 2, Table 2). Below that depth, $^{10}Be/^{9}Be$ ratios are not considered reliable because of the low ^{10}Be concentrations of the samples together with uncertainties induced by the blank correction; therefore the constant Co-flux model was applied. This model gives growth rates (1.5–2.3 mm/Ma) for the older part of the crust that are similar to those of the younger part (Tables 1 and 2). The growth rate determination for the upper part of crust Marshalls (0–17.5 mm) is also based on the best fit of the measured $^{10}Be/^{9}Be$ ratios (1.67 mm/Ma). In the lower part, the growth rate derived from the constant Co-flux model is higher (1.3–5.0 mm/Ma, Table 2). The $^{10}Be/^{9}Be$ ratio for a surface scraping of crust Tasman ($1.21 \pm 0.25 * 10^{-7}$) is identical within error to a previously measured ratio ($1.14 \pm 0.09 * 10^{-7}$; *von Blanckenburg et al.* [1996a]). Note that any reported age older than 10 Myr has a large uncertainty arising from the dating technique. Conservative error estimates are in the order of 10 ± 1 Ma, 20 ± 2 Ma, and 30 ± 5 Ma, although previous work has shown that age models in ferromanganese crusts often yield a good match with precisely dated events [e.g., *Frank*, 2002]. However, due to these uncertainties in dating, no attempt will be made to determine the absolute timing of any event; only the general trends and evolution will be discussed.

4.2. Lead Isotope Data

[19] High precision Pb isotopic compositions were determined for 53 samples from crust Tasman, 49 samples from crust Nova, and 48 samples from crust Marshalls (Table 3[1]; Figures 3, 4, and 5).

[20] The Pb isotope surface values for crust Tasman are consistent with previously published data by *von Blanckenburg et al.* [1996b], and the surface data for crust Marshalls are similar to other equatorial Pacific crusts from the same water depth (1800–2300 m; *Ling et al.* [1997]). Strikingly similar Pb isotope time series trends exist for crusts Tasman and Nova, even though their locations are separated by more than 27° of latitude (> 3000 km) and 5000 m of water depth (Figure 1). The only major offset between the records of the two crusts is the different age of the start of the decrease in $^{206}Pb/^{204}Pb$ and $^{208}Pb/^{204}Pb$, which is around 17 Ma in crust Nova and around 10 Ma in crust Tasman. The similarity is even more striking when comparing these two records with the time series from the Marshalls crust. As shown in Figure 4, the Pb isotope time series of this crust is essentially identical to published data for other crusts from the equatorial Pacific, but clearly different from crusts Nova and Tasman. Another important observation from comparison of the data in Figure 4 is that the difference between crusts Nova and equatorial Pacific deep water records was small between 40 and 30 Ma, significantly larger afterward, but then converged again from about 10 Ma. The latter two statements also apply to crust Tasman, which shows similar values to crust Nova over the past 23 Myr.

[21] Considering recently published data for ferromanganese crust time series from the Southern Ocean [*Frank et al.*, 2002], the difference in Pb isotopic composition between

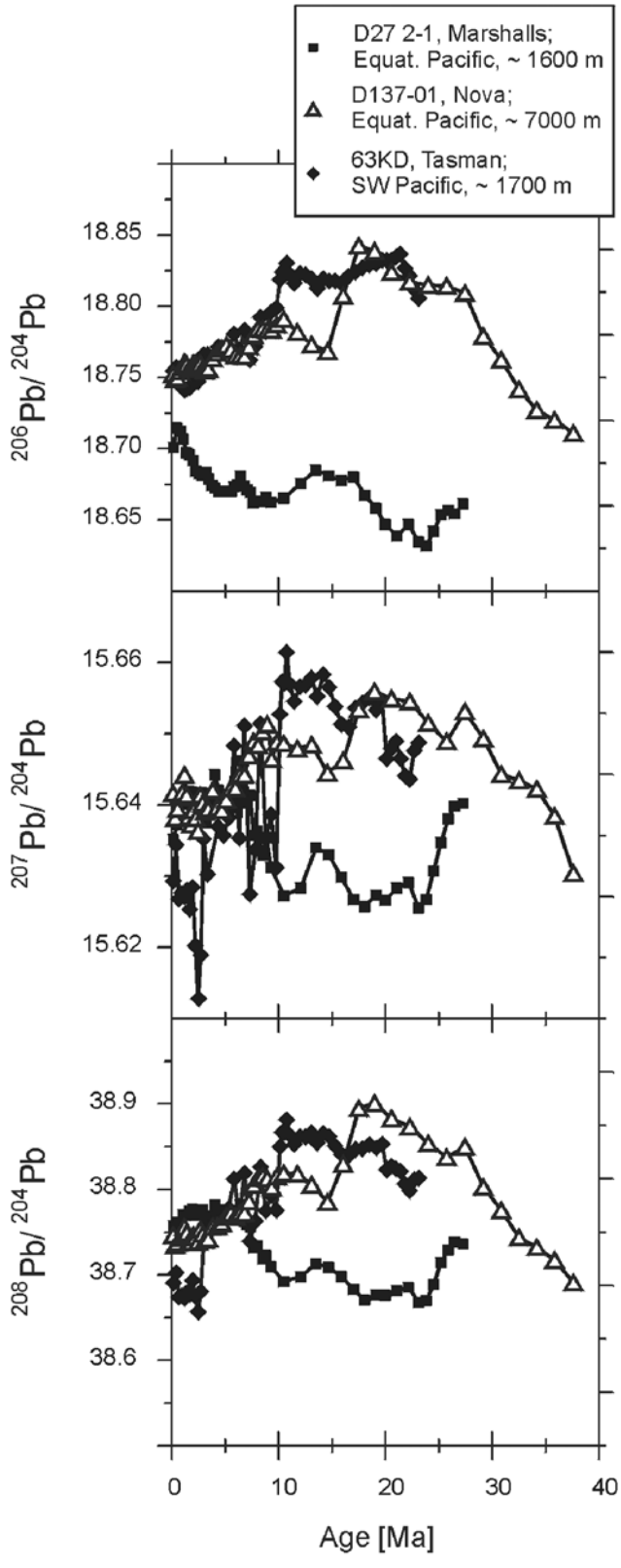

Figure 3. $^{206}Pb/^{204}Pb$, $^{207}Pb/^{204}Pb$, and $^{208}Pb/^{204}Pb$ time series derived from crusts Marshalls (filled squares), Nova (open triangles), and Tasman (filled diamonds). Two-sigma error bars are smaller than the symbols.

crusts Tasman and Nova, compared with equatorial Pacific deep water, are likely to have been caused by larger amounts of admixed Southern Ocean waters (Figure 4). This is in agreement with the southern location of crust Tasman (28°S) and the deep water location of crust Nova in the southern equatorial Pacific. Further supporting evidence comes from Pb-Pb mixing diagrams (Figure 5), where both the Tasman and Nova records plot between equatorial Pacific deep water and Southern Ocean water. Crust Marshalls is essentially identical to the other equatorial Pacific deep water records. Therefore it is not discussed further and Nd isotope analyses were not carried out.

4.3. Neodymium Isotope Data

[22] Neodymium isotope time series for crusts Tasman and Nova are shown in Figure 6 and exhibit different amplitudes of change. While crust Nova, recording equatorial Pacific bottom water, varies only by 1.5 ε units, crust Tasman from the deep southwest Pacific displays one of the largest ranges in ε_{Nd} known for ferromanganese crust time series (2.8 ε units; Figure 6). In agreement with the Pb isotope patterns, the Nd isotope time series from the deep southwest Pacific plots between Southern Ocean water and equatorial Pacific deep water prior to 10 Ma (Figure 6), and exhibits a major shift toward higher ε_{Nd} values that started around 10 Ma. The present-day Nd isotopic composition is within error indistinguishable from equatorial Pacific deep water. In contrast, Nd from the Nova Canton Trough crust displays an isotopic composition intermediate between equatorial Pacific deep water and Southern Ocean water over the entire 38 Myr growth period (Figure 6). In detail, a trend toward lower values occurs for samples between 38 and ~20.5 Ma and a reverse trend for those from ~17 Ma onward, in line with those exhibited by $^{206}Pb/^{204}Pb$ at the same location (Figures 3 and 4).

5. Discussion

[23] One of the most important results exhibited by the two investigated time series from equatorial Pacific bottom water and southwest Pacific deep water, is that Nd and Pb isotope time series at both locations clearly reflect a mixture of Southern Ocean water and equatorial Pacific deep water. Superimposed on the general picture of mixing of two water masses, the Nd and Pb isotope records contain more detailed information about paleoceanographic changes that occurred in the South Pacific during the Cenozoic, which are specific for each location and will be discussed next.

5.1. Evolution of Equatorial Pacific Bottom Water

[24] The Nova Canton Trough represents an ideal location to study the Cenozoic mixing history of equatorial Pacific bottom water for several reasons. First, the anomalous depth of Nova Canton Trough of 7000 to 8400 m constrains the bottom water composition to be modified AABW in the equatorial Pacific. Furthermore, the Nova Canton Trough represents a tectonically stable area since its formation in the Early Cretaceous [see *Larson et al.*, 2002, and references therein]. In addition, the location is very remote and hence it is highly unlikely that the radiogenic isotope

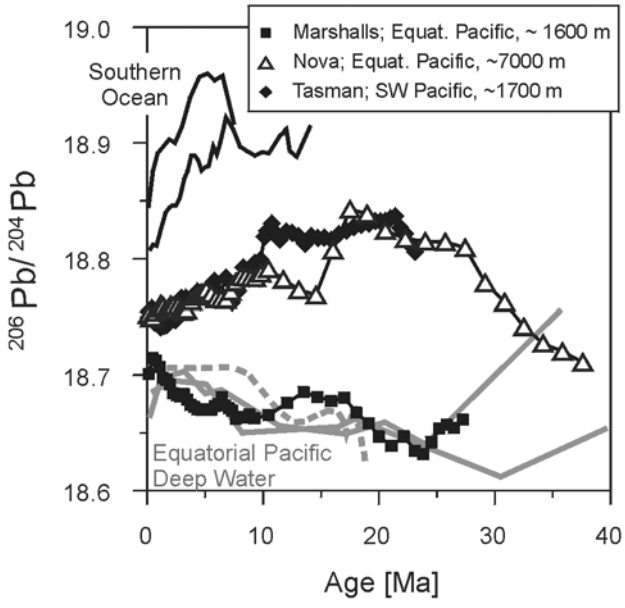

Figure 4. $^{206}Pb/^{204}Pb$ versus age for crusts Marshalls, Nova, and Tasman. Shown for comparison are equatorial Pacific records derived from crusts D11-1, CD29-2 (solid gray lines; 1800–2300 m water depth; *Ling et al.* [1997]), and VA13/2 (dashed gray line, 4800 m water depth; *Ling et al.* [1997]), and Southern Ocean records (solid black lines; *Frank et al.* [2002]).

composition of its bottom water is influenced by erosional inputs from continents or volcanic arcs. Therefore Nd and Pb isotopes monitor the undisturbed history of imported and admixed water masses.

5.1.1. Present-Day Oceanographic Setting for Crust Nova

[25] The radiogenic isotope signature of deep and bottom waters in the equatorial and southern Pacific, as recorded by ferromanganese crusts, monitors the deep water flow path as outlined in section 2. Contemporary Southern Ocean waters south of Australia have a $^{206}Pb/^{204}Pb$ isotopic composition of 18.80–18.82 [*Abouchami and Goldstein*, 1995; *Frank et al.*, 2002] and an ε_{Nd} of −7.6 to −8.2 [*Albarède et al.*, 1997; *Frank et al.*, 2002]. The DWBC east of New Zealand, more precisely east of the Campbell Plateau, already exhibits a lower $^{206}Pb/^{204}Pb$ isotopic composition of ~18.77 and a relatively high ε_{Nd} of −7.6 [*Baker et al.*, 2001; *Ulfbeck et al.*, 2001]. Further north, crust Nova from the southern equatorial Pacific (7000 m water depth) can be considered to have the most Pacific-like composition with a $^{206}Pb/^{204}Pb$ ratio of 18.75 and an ε_{Nd} of −5.5. These data demonstrate a continuous northward dilution of Southern Ocean water with overlying Pacific deep water ($^{206}Pb/^{204}Pb$ = 18.66–18.70, ε_{Nd} = −3.0 to −3.7; *Ling et al.* [1997] and this study), leading to progressively more radiogenic Nd isotopes and more central-Pacific like Pb isotopes. Regarding its present-day Nd isotopic composition, equatorial Pacific bottom water consists roughly of a 1:1 mixture of Southern Ocean water and overlying equatorial Pacific deep water. This is also true for Pb isotopes, and confirms the suitability of Pb isotopes as a circulation tracer at remote locations.

5.1.2. Paleoceanography for Crust Nova

[26] The new Nd and Pb isotope time series of crust Nova will be used in the following to reconstruct the history of export of Southern Ocean Water to the equatorial Pacific. The records will be discussed in two time-intervals, corresponding to (1) the build up of the ACC (~38 to ~21/17 Ma), and (2) the build up of the East Antarctic Ice Sheet (~17 Ma until present-day), both of which led to distinct changes in the Pb and Nd isotopic composition of equatorial Pacific bottom water.

5.1.2.1. Buildup of the ACC: 38 to 21/17 Ma

[27] During the Eocene (~38 Ma), the Nd isotope signature of equatorial Pacific bottom water was close to and Pb isotopes were identical to the signature of equatorial Pacific deep water (Figures 4 and 6). This indicates efficient water mass exchange at that time, and implies no major export of AABW to the Pacific sector prior to the Eocene/Oligocene boundary. From then onward, Nd and Pb isotope trends in crust Nova are consistent with an increased or starting admixture of Southern Ocean water to equatorial Pacific bottom water. This is suggested by a decrease in ε_{Nd} from −5.3 to −6.8 from 38 to 21 Ma, and an increase in $^{206}Pb/^{204}Pb$ ratios from 18.71 to 18.84 from 38 to 17.5 Ma (Figures 3, 4, and 6). Such an increased import of southern water masses is likely to have occurred

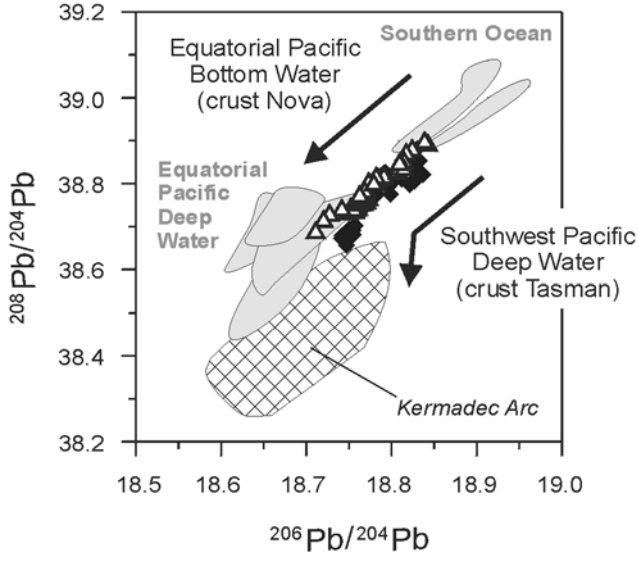

Figure 5. $^{206}Pb/^{204}Pb$ versus $^{208}Pb/^{204}Pb$. Crusts Tasman and Nova display well-defined trends with age. Arrows qualitatively indicate the individual trends of the two crusts. Omitting the past 3 Myr for crust Tasman, indicated by the kink in the arrow, the data for both crusts plot between Southern Ocean water [*Frank et al.*, 2002] and equatorial Pacific deep water (*Ling et al.* [1997] and this study). The trend for crust Tasman over the past 3 Myr evolves toward the composition of the Kermadec Arc (data source: GEOROC global geochemical database, http://georoc.mpch-mainz.gwdg.de/).

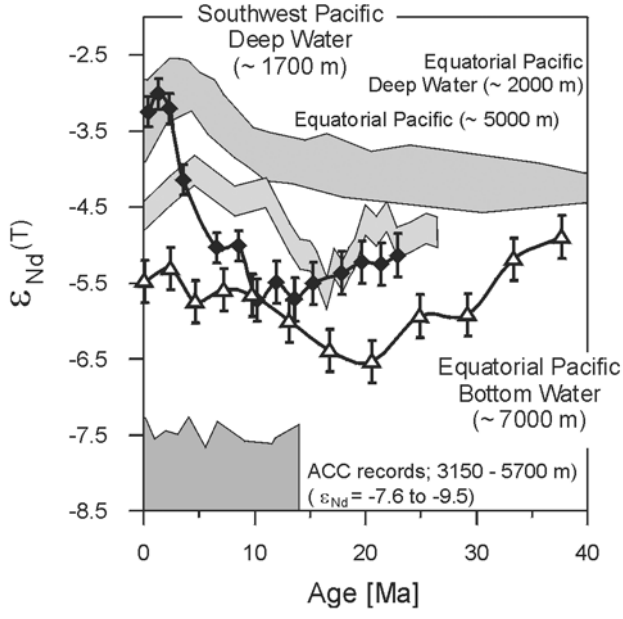

Figure 6. Neodymium isotope data versus age for crusts Nova (open triangles) and Tasman (filled diamonds) compared with equatorial Pacific records [*Ling et al.*, 1997] and Southern Ocean records [*Frank et al.*, 2002] (shaded fields).

within the DWBC, the evolution of which has ultimately been coupled to the build up of the ACC [*Carter et al.*, 1999]. The initial step to establishing the ACC in the Pacific sector was the opening of the Tasmanian gateway between Australia and Antarctica, which occurred in the late Eocene between 37 Ma for shallow water and 33.5 Ma for deep water due to the rapid northward movement of Australia away from Antarctica [e.g., *Kennett and von der Borch*, 1986; *Exon et al.*, 2002]. The onset of deep water inflow into the Pacific through this gateway led to the inception of the ACC related bottom water circulation in this segment of the Southern Ocean, e.g., the export of Southern Ocean water to the Pacific, most likely within the DWBC as indicated by the widespread occurrence of Oligocene hiatuses in deep ocean sediments east of New Zealand [e.g., *Kennett*, 1977; *Carter and McCave*, 1994; *Exon et al.*, 2001].

[28] The circumpolar route of the ACC was completed by the opening of Drake Passage between South America and Antarctica to deep water exchange between the Pacific and Atlantic Oceans. The exact timing of the opening is controversial and estimates for the development of an intermediate- to deep water passage range from the Eocene/Oligocene boundary (33.5 Ma) to as young as 22–17 Ma [*Barker and Burrell*, 1977; *Beu et al.*, 1997; *Lawver and Gahagan*, 1998; *Barker*, 2001; *Pfuhl et al.*, 2002; *Latimer and Filippelli*, 2002; *Lawver and Gahagan*, 2003; *Scher and Martin*, 2003].

[29] Interpreting the gradual decrease in Nd- and increase in Pb isotope data in crust Nova from 38 to 21/17 Ma in terms of an increased import of southern water masses is based on the assumption that Oligocene Southern Ocean water exhibited a similar Nd isotopic composition as that of Southern Ocean water over the past 14 Myr (Figure 6). This is, however, equivocal because *Scher and Martin* [2003] recently reported fish teeth analyses from Site 1090 in Cape Basin that exhibit a decreasing Nd isotopic composition of Southern Ocean water through the Oligocene. Taking these data into account, it may well be that the observed gradual decrease in ε_{Nd} in crust Nova is a result of a combined change in both the composition and the flux of Southern Ocean water entering the deep Pacific. A change in the source composition alone cannot fully explain our data because that would require the signal observed in Cape Basin to be delivered to the Equatorial Pacific without significant mixing with overlying Pacific deep water.

5.1.2.2. Consequences of the Buildup of the East Antarctic Ice Sheet (EAIS): 17 to 0 Ma

[30] The above described trends in Pb and Nd isotopes toward a higher influence of Southern Ocean water masses terminated in the middle Miocene. Between 17.5–16.0 Ma and 20.5–16.8 Ma, the Pb and Nd isotope patterns respectively show a turning point, resulting in opposite trends to those observed for earlier times (Figures 3, 4, and 6). This indicates a reorganization of Pacific circulation patterns, most likely caused by major paleoceanographic changes occurring in the middle Miocene, such as build up of the EAIS or closure of the Indonesian gateway. Expansion of the Antarctic cryosphere entailed increased production and export of AABW and significant deep ocean cooling [e.g., *Shackleton and Kennett*, 1975; *Kennett and von der Borch*, 1986; *Miller et al.*, 1987; *Woodruff and Savin*, 1989; *Wright et al.*, 1992; *Flower and Kennett*, 1995; *Billups and Schrag*, 2002; *Hall et al.*, 2003]. At first glance it may seem contradictory that the most Southern Ocean-like Nd and Pb isotope values were reached at 20 Ma, directly after the onset of the ACC, and that increased export of Antarctic Bottom water around 15 Ma resulted in more Pacific-like Pb and Nd isotopes in equatorial Pacific bottom water. Our favored explanation for this is an overall strengthening of Pacific circulation at deep and intermediate water depths, thereby producing more vigorous circulation and mixing. A general stimulation of thermohaline circulation as a consequence of the presence of the east Antarctic ice cap has also been suggested by *Exon et al.* [2001] based on evidence from ODP Leg 181. This hypothesis is consistent with the closure of the Indonesian gateway around the same time, which curtailed direct export of deep water from the Pacific Ocean to the Indian Ocean, and probably led to a reorganization and amplification of Pacific circulation patterns (see section 5.2.2).

5.2. Evolution of Southwest Pacific Deep Water

[31] The above results demonstrate that Nd and Pb isotope studies of deep waters from remote locations in the oceans can be used to reconstruct circulation patterns. The setting in the southwest Pacific is more complex for several reasons. First, crust Tasman was recovered from a much shallower water depth than crust Nova (1700 m compared to ~7000 m). Second, the Pb isotopes in crust Tasman indicate a slight change in input sources to the Lord Howe Rise over the past 3 Myr (Figures 3,5). Third,

changes in the oceanographic setting of crust Tasman over the past 23 Myr obviously entailed large changes in ε_{Nd} (Figure 6), which are not observable in crust Nova because of growth from a different water mass.

5.2.1. Present-Day Oceanographic Setting for Crust Tasman

[32] Data for the surface layer of crust Tasman provide the modern radiogenic isotope signature for the deep southwest Pacific and show Nd isotope characteristics ($\varepsilon_{Nd} = -3.4$) identical to equatorial Pacific deep water as derived from ferromanganese crusts (e.g., $\varepsilon_{Nd} = -3.0$ to -3.7, *Ling et al.* [1997]; $\varepsilon_{Nd} = -2.8$ to -4.5, *Aplin et al.* [1986]). In contrast to the present-day Nd isotope signature, the $^{206}Pb/^{204}Pb$ ratio of 18.76 indicates mixing between Southern Ocean water ($^{206}Pb/^{204}Pb$ = 18.80–18.82; *Abouchami and Goldstein* [1995]; *Frank et al.* [2002]) and equatorial Pacific deep water ($^{206}Pb/^{204}Pb$ = 18.66–18.70; *Ling et al.* [1997] and this study). However, considering the relatively low $^{207}Pb/^{204}Pb$ and $^{208}Pb/^{204}Pb$ ratios ($^{207}Pb/^{204}Pb$: 15.629, $^{208}Pb/^{204}Pb$: 38.690), it is likely that the Pb isotopic signature in the southwest Pacific has been modified by a local source. In Pb-Pb mixing plots (Figure 5), the data prior to 3 Ma describe a linear array between Southern Ocean water and equatorial Pacific deep water that is parallel to the one observed for crust Nova. A kink in the trend occurs at about 3 Ma, pointing to the influence of an additional end-member characterized by low $^{207}Pb/^{204}Pb$ and $^{208}Pb/^{204}Pb$ ratios. We suggest that this signal is derived from one of the local volcanic arcs (see below). In summary, the Nd isotope data are not only consistent with the present-day deep water circulation pattern as outlined in section 2, but definitively require supply of deep water to the southwest Pacific from the equatorial Pacific, whereas present-day Pb isotopes are overprinted by a local source.

5.2.2. Paleoceanography in the Southwest Pacific

[33] No work has been carried out to address past deep water circulation pattern in the area west of New Zealand. Since our Nd isotope data provide reliable information about the present-day circulation pattern, it is used to construct possible scenarios for changes in the paleoceanography of that area. However, the possibility of overprinting of the Nd isotopic composition by local sources must first be excluded.

5.2.2.1. Potential Source Variations

[34] It is unlikely that significant detrital or dissolved material supplied by Australian rivers reaches the location of crust Tasman based on bathymetric considerations (Figure 1). Between Lord Howe Rise and the Australian continent exists the deep Tasman Sea and the largest river of eastern Australia, the Murray, drains into the Great Australian Bight further south. Furthermore, the Nd isotopic composition of the Murray ($\varepsilon_{Nd} = -4.7$; *Goldstein and Jacobsen* [1988]) is lower than that of seawater and therefore cannot serve as an end-member for the upward trend in ε_{Nd} over the past 10 Myr.

[35] Eolian dust must also be considered as a potential influence. Due to the northward drift of Australia, aridification has progressively increased the supply of windblown material over the past 10 Myr, most significantly since 5 Ma [*Exon et al.*, 2002]. Australian dust exhibits a relatively low (unradiogenic) Nd isotopic composition ($\varepsilon_{Nd} = -3.7$ to -11.7; *Grousset et al.* [1992]). Increased dust input should therefore drive the Nd isotope evolution in the direction opposite to that observed, so eolian continental input can also be excluded as a suitable explanation for the observed shift in ε_{Nd} from -5.7 to -2.9 between 10 Ma and present-day in crust Tasman.

[36] Volcanic exhalations can also be excluded as potential drivers because the number of ash layers in DSDP cores on Lord Howe Rise suggest that middle and early late Miocene volcanism was much more prominent than Quaternary volcanism in this sector of the southwest Pacific [*Gardner et al.*, 1986].

[37] This leaves erosion of local arcs as the only potential overprinting candidate. According to *Ballance* [1999], Neogene arc activity began simultaneously at 25 Ma in different areas and experienced a major reorganization and simplification around 15 Ma [*Herzer*, 1995]. Ten Myr of arc stability without back-arc formation followed that period, and from 5 Ma onward another major reorganization has been taking place [*Ballance*, 1999]. The arcs in the southwest Pacific typically show ε_{Nd} values of +5 to +10 (for a compilation of data see the GEOROC global geochemical database; http://georoc.mpch-mainz.gwdg.de/). Although this range of isotopic compositions and the history of arc evolution fits with the observed trend in crust Tasman data because the major increase in ε_{Nd} started between 6.6 and 3.6 Ma (Figure 6), there are strong arguments against a progressive increase in arc erosion over the past 10 Myr. If eroded arc material is considered a potential driver for the huge shift in the Nd isotopic composition Pb isotopes should display this influence even more strongly because of the shorter residence time of Pb, which makes it more sensitive to local inputs. The general trend in Pb-Pb mixing plots (Figure 5), however, only points to a potential arc end-member (e.g., Kermadec arc) for the past 3 Myr. This is due to a significant drop in the $^{208}Pb/^{204}Pb$ and $^{207}Pb/^{204}Pb$ ratios around 3 Ma, which clearly requires the contribution of an arc-like source from that time onward. In contrast, the upward Nd isotope trend ceased at $\sim$1.3 Ma even though the arc end-member isotopic composition for Nd was not closely approached. Furthermore, the trend in ε_{Nd} ceases at exactly the point at which the isotopic composition of equatorial Pacific deep water is reached (Figure 6). Although we cannot conclusively exclude a contribution from local arcs to the Nd isotope signal, it is very unlikely that they were responsible for the observed changes.

[38] Finally, we must consider the possibility that the large shift in ε_{Nd} was caused by a change in paleodepth of the crust Tasman site, potentially causing movement into a different water mass. Several studies indicate, however, a relatively unchanged paleodepth for different DSDP sites on Lord Howe Rise since the late Oligocene (difference in depth is less than 100 m; *Sclater et al.* [1985]; *Ayress*, [1994]; *Flower and Kennett* [1995]; *Gaina et al.* [1998]).

5.2.2.2. Effects of the Closure of the Indonesian Gateway

[39] Having excluded other potential processes, the large shift in Nd isotopes likely reflects changes in

paleocirculation. We propose that prior to 10 Myr deep water over Lord Howe Rise was sourced from two different regions: the equatorial Pacific and the Southern Ocean. This is in accordance with the Pb and Nd isotope evidence for the time interval 23–10 Ma and also fits data for crust Nova. Supporting evidence comes from the fact that Lord Howe Rise moved northward together with the Australian plate and the location of crust Tasman was about 8° further south at 25 Ma [*Sclater et al.*, 1985].

[40] From 10 Ma onward, equatorial Pacific deep water became progressively more dominant for the crust Tasman location in the southwest Pacific, resulting in a present-day Nd isotopic composition identical to that of equatorial Pacific deep water. Consequently, either the deep current supplying the southwest Pacific must have been strengthened, or the Southern Ocean water supply/source must have become less important. Here we suggest that the major change in ε_{Nd} on Lord Howe Rise was driven by closure of the Indonesian Seaway and subsequent reorganization of circulation in the southwest Pacific. It is very likely that the existence of the present-day southward deflection of the deeper parts of the SEC (Figure 1) that supplies an equatorial Pacific Nd isotopic composition to the basins east of Lord Howe Rise is a result of the closure of the Indonesian gateway. Reconstructions by *Kennett et al.* [1985] also indicate that in the early Miocene (~20 Ma) the SEC was the main current flowing from the Pacific to the Indian Ocean. Due to the general motion of southwest Pacific plates (westward), the Australian plate (northward), and the Eurasian plate (fixed), an up to 1300 km wide seaway existed at that time between Indonesian and Australian landmasses. Based on planktonic foraminiferal biogeography, *Kennett et al.* [1985] estimated that this pathway has been shallowing/restricting since the middle Miocene. This is in line with assessments based on radiolarian studies, which indicate closure of the Indo-Pacific passage to significant (deep) westward flow between 12 and 10 Ma [*Romine and Lombari*, 1985]. The tectonic history of the region allows estimates ranging from 15.5 to 7.5 Ma for the closure of the Indonesian seaway to deep water exchange [e.g., *Linthout et al.*, 1997; *Nishimura and Suparka*, 1997; *Tsuchi*, 1997]. No matter what the exact timing of the closure, it clearly had severe effects on Pacific Ocean circulation, as can be seen from our Nd isotope record from crust Tasman. Moreover, a general strengthening of the oceanic gyre system probably took place at the same time due to a steepening of the latitudinal temperature gradients (see section 5.1.2). These conclusions are supported by a study of *Kennett et al.* [1985], who proposed that an ''interlocking'' between the Indonesian and New Guinea landmasses in the middle Miocene caused a pile-up of westward flowing equatorial currents, mainly the SEC, resulting in initiation of the Equatorial Undercurrent (EUC) as a return flow from the western equatorial Pacific to the eastern equatorial Pacific (see Figure 1). *Godfrey* [1996] suggested that the closure of the Indonesian throughflow also resulted in strengthening of the East Australian Current, though the timing slightly lagged the closure of the gateway. Major reorganization of the paleoenvironment in the southwest Pacific due to the closure of the Indonesian gateway was also recorded on northeastern Australian carbonate platforms [e.g., *McKenzie and Davies*, 1993]. It is interesting to note that according to paleogeographic reconstructions, *Lee and Lawver* [1995] suggested a restriction of the flow of the SEC prior to ~5 Ma and a total blockage around 4.4 Ma, the time of major orogeny in New Guinea. This is consistent with *Wei* [1998], who proposed a southward shift of the Tasman Front at 4.4 Ma. Both findings are in agreement with the major changes in Nd isotopic compositions in the southwest Pacific occurring between 6.6 and 3.6 Ma (Figure 6) and strengthen the proposition that the rise in ε_{Nd} on Lord Howe Rise has been due to the southward deflection of the SEC during closure of the Indonesian Seaway.

6. Conclusions

[41] We demonstrate that the Nd and Pb isotopic compositions of equatorial Pacific bottom water and southwest Pacific deep water can be identified in two ferromanganese crusts and those can be used in time series to reconstruct Cenozoic circulation patterns. For two sites in the southern equatorial Pacific (Nova Canton Trough) and southwest Pacific (Lord Howe Rise), both isotope systems delineate in general a mixing of equatorial Pacific deep water and Southern Ocean water over the past 38 and 23 Myr, respectively. Overprint of Nd and Pb isotope signatures by local sources (e.g., continental inputs or arc weathering) can be excluded for the record from the Nova Canton Trough and is highly unlikely for the record from Lord Howe Rise prior to 3 Myr.

[42] The evolution of Pb and Nd isotopes in equatorial Pacific bottom water documents increased export of Southern Ocean water carried by the Deep Western Boundary Current as a result of the progressive build up of the ACC from 38 to 21/17 Ma due to the opening of the Tasmanian gateway and the Drake Passage. There may also have been a change in the isotopic composition of Southern Ocean water during the Oligocene that added to the observed signal [*Scher and Martin*, 2003]. From 17 Ma to the present, development of the East Antarctic Ice Sheet initiated an increased production and export of Antarctic Bottom Water, which in turn led to more vigorous Pacific circulation and mixing. This effect was, moreover, enhanced by the closure of the Indonesian gateway. While the impact of the cessation of export of deep water from the Pacific to the Indian Ocean in the middle Miocene is not very prominent in the deep Nova Canton Trough, which is dominated by inflowing modified Antarctic Bottom Water, it markedly changed the Nd isotope pattern in the southwest Pacific. Today, deep water enters the southwest Pacific from the north, as a southward deflection of the South Equatorial Current, which delivers an equatorial Pacific-like Nd isotopic composition. This current, however, was probably only established in the course of the closure of the Indonesian seaway, since Nd isotopes prior to 10 Ma clearly suggest a stronger Southern Ocean-like influence or/and a weaker equatorial Pacific influence.

[43] Overall, comparison of published Pb and Nd isotope records from the equatorial and southern Pacific Ocean display small relative differences in the Eocene and early

Oligocene, larger differences in the Oligocene through middle Miocene, and then merge again toward present-day. This is consistent with (1) a common source and strong equatorially dominated circulation patterns in the Eocene with no major export of AABW, increased production and export of AABW to the Pacific, (2) from the Oligocene onward due to the build up of the Antarctic Circumpolar Current coupled with generally weak circulation and water mass exchange, leading to more distinct isotopic signatures for the south and equatorial Pacific regions, and (3) more intense Pacific circulation since the middle Miocene as a consequence of major climatic and paleogeographic changes forcing the southern and equatorial records to become more similar again. Although our results provide important new information for the reconstruction of Eocene through Miocene deep water circulation, more records of radiogenic isotopes at higher time-resolution from remote locations and different water depths are needed to achieve a comprehensive reconstruction of past circulation patterns in the Pacific Ocean.

[44] **Acknowledgments.** H. Baur, U. Menet, D. Niederer, F. Oberli, B. Rütsche, and A. Süsli are gratefully acknowledged for providing assistance with technical problems. M. Meier is thanked for help in setting up the Nd chemistry. Special thanks go to M. Rehkämper and D.-C. Lee for advice in chemistry, mass spectrometry, and for many fruitful discussions. We would like to acknowledge M. Andres, J. A. McKenzie, D. Schmidt, and H. Weissert, who improved this paper by providing constructive comments on ideas about the paleoceanography in the South Pacific, and B. Reynolds for comments on an earlier version of this manuscript. We thank Scripps Institute of Oceanography for supplying crust Nova D137. H. D. Scher is thanked for a very constructive review. This research was funded by the Schweizerische Nationalfonds (SNF).

References

Abouchami, W., and S. L. Goldstein (1995), A lead isotopic study of Circum-Antarctic manganese nodules, *Geochim. Cosmochim. Acta*, *59*, 809–820.

Abouchami, W., S. L. Goldstein, S. J. G. Galer, A. Eisenhauer, and A. Mangini (1997), Secular changes of lead and neodymium in central Pacific seawater recorded by a Fe-Mn crust, *Geochim. Cosmochim. Acta*, *61*, 3957–3974.

Albarède, F., S. L. Goldstein, and D. Dautel (1997), The neodymium isotopic composition of manganese nodules from the Southern and Indian oceans: The global oceanic neodymium budget, and their bearing on deep ocean circulation, *Geochim. Cosmochim. Acta*, *61*, 1277–1291.

Aplin, A., A. Michard, and F. Albarède (1986), $^{143}Nd/^{144}Nd$ in Pacific ferromanganese encrustations and nodules, *Earth Planet. Sci. Lett.*, *81*, 7–14.

Axelsson, M. D., I. Rodushkin, J. Ingri, and B. Öhlander (2002), Multielemental analysis of Mn-Fe nodules by ICP-MS: Optimisation of analytical method, *Analyst*, *127*, 76–82.

Ayress, M. A. (1994), Cainozoic palaeoceanographic and subsidence history of the eastern margin of the Tasman Basin based on Ostracoda, in *Evolution of the Tasman Sea*, edited by G. J. van der Lingen et al., pp. 139–157, A. A. Balkema, Brookfield, Vt.

Baker, J. A., T. E. Waight, I. J. Graham, and I. C. Wright (2001), High resolution Pb isotopic profiles of Fe-Mn nodules (19-0 Ma) from the deep western boundary current, southern Pacific, *Eos Trans. AGU*, *82*(47), Fall Meet. Suppl., Abstract OS31C-0438.

Ballance, P. F. (1999), Simplification of the Southwest Pacific Neogene arcs: Inherited complexity and control by a retreating pole of rotation, *Geol. Soc. Spec. Publ.*, *164*, 7–19.

Barker, P. F. (2001), Scotia Sea regional tectonic evolution: Implications for mantle flow and palaeocirculation, *Earth Sci. Rev.*, *55*, 1–39.

Barker, P. F., and J. Burrell (1977), The opening of the Drake Passage, *Mar. Geol.*, *25*, 15–34.

Beu, A. G., M. Griffin, and P. A. Maxwell (1997), Opening of Drake Passage and Late Miocene to Pleistocene cooling reflected in Southern Ocean molluscan dispersal: Evidence from New Zealand and Argentina, *Tectonophysics*, *281*, 83–97.

Billups, K., and D. P. Schrag (2002), Paleotemperatures and ice volume of the past 27 Myr revisited with paired Mg/Ca and $^{18}O/^{16}O$ measurements on benthic foraminifera, *Paleoceanography*, *17*(1), 1003, doi:10.1029/2000PA000567.

Broecker, W. S. (1991), The Great Ocean Conveyor, *Oceanography*, *4*, 79–89.

Broecker, W. S., and T. H. Peng (1982), *Tracers in the Sea*, 690 pp., Lahmont-Doherty Earth Observatory, Palisades, N. Y.

Carter, L., and I. N. McCave (1994), Development of sediment drifts approaching an active plate margin under the SW Pacific Deep Western Boundary Current, *Paleoceanography*, *9*, 1061–1085.

Carter, L., and J. Wilkin (1999), Abyssal circulation around New Zealand—A comparison between observations and a global circulation model, *Mar. Geol.*, *159*, 221–239.

Carter, R. M., et al. (1999), *Proceedings of the Ocean Drilling Program*, *Initial Reports*, vol. 181, Ocean Drill. Program, College Station, Tex.

Christensen, J. N., A. N. Halliday, L. V. Godfrey, J. R. Hein, and D. K. Rea (1997), Climate and ocean dynamics and the lead isotopic records in Pacific ferromanganese crusts, *Science*, *277*, 913–918.

Claude-Ivanaj, C., A. W. Hofmann, I. Vlastélic, and A. Koschinsky (2001), Recording changes in ENADW composition over the last 340 ka using high-precision lead isotopes in a Fe-Mn crust, *Earth Planet. Sci. Lett.*, *188*, 73–89.

Cochran, J. K., T. McKibbin-Vaughan, M. M. Dornblaser, D. Hirschberg, H. D. Livingston, and K. O. Buesseler (1990), ^{210}Pb scavenging in the North Atlantic and North Pacific Oceans, *Earth Planet. Sci. Lett.*, *97*, 332–352.

Cohen, A. S., R. K. O'Nions, R. Siegenthaler, and W. L. Griffin (1988), Chronology of the pressure-temperature history recorded by a granulite terrain, *Contrib. Mineral. Petrol.*, *98*, 303–311.

Craig, H., S. Krishnaswami, and B. L. K. Somayajulu (1973), Radioactive disequilibrium in the deep sea, *Earth Planet. Sci. Lett.*, *17*, 295–305.

Exon, N. F., et al. (2001), *Proceedings of the Ocean Drilling Program*, *Initial Reports*, vol. 189, Ocean Drill. Program, College Station, Tex.

Exon, N. F., et al. (2002), Drilling reveals climatic consequences of Tasmanian gateway opening, *Eos Trans. AGU*, *83*(23), 253, 258–259.

Flower, B. P., and J. P. Kennett (1995), Middle Miocene deepwater paleoceanography in the southwest Pacific: Relations with East Antarctic Ice Sheet development, *Paleoceanography*, *10*, 1095–1112.

Frank, M. (2002), Radiogenic isotopes: Tracers of past ocean circulation and erosional input, *Rev. Geophys.*, *40*(1), 1001, doi:10.1029/2000RG000094.

Frank, M., R. K. O'Nions, J. R. Hein, and V. K. Banakar (1999a), 60 Myr records of major elements and Pb-Nd isotopes from hydrogenous ferromanganese crusts: Reconstruction of seawater paleochemistry, *Geochim. Cosmochim. Acta*, *63*, 1689–1708.

Frank, M., B. C. Reynolds, and R. K. O'Nions (1999b), Nd and Pb isotopes in Atlantic and Pacific water masses before and after closure of the Panama gateway, *Geology*, *27*, 1147–1150.

Frank, M., N. Whiteley, S. Kasten, J. R. Hein, and K. O'Nions (2002), North Atlantic Deep Water export to the Southern Ocean over the past 14 Myr: Evidence from Nd and Pb isotopes in ferromanganese crusts, *Paleoceanography*, *17*(2), 1022, doi:10.1029/2000PA000606.

Gaina, C., D. R. Müller, J.-Y. Royer, J. Stock, J. Hardebeck, and P. Symonds (1998), The tectonic history of the Tasman Sea: A puzzle with 13 pieces, *J. Geophys. Res.*, *103*(B6), 12,413–12,433.

Galer, S. J. G., and W. Abouchami (1998), Practical application of lead triple spiking for correction of instrumental mass discrimination, *Mineral. Mag.*, *62A*, 491–492.

Gardner, J. V., C. S. Nelson, and P. A. Baker (1986), Distribution and character of pale green laminae in sediment from Lord Howe Rise: A probable late Neogene and Quaternary tephrostratigraphic record, *Initial Rep. Deep Sea Drill. Proj.*, *90*, 1145–1159.

Godfrey, J. S. (1996), The effect of the Indonesian throughflow on ocean circulation and heat exchange with the atmosphere: A review, *J. Geophys. Res.*, *101*(C5), 12,217–12,237.

Goldstein, S. J., and S. B. Jacobsen (1988), Nd and Sr isotopic systematics of river water suspended material: Implications for crustal evolution, *Earth Planet. Sci. Lett.*, *87*, 249–265.

Grousset, F. E., P. E. Biscaye, M. Revel, J.-R. Petit, K. Pye, S. Joussaume, and J. Jouzel (1992), Antarctic (Dome C) ice-core dust at

18 k.y. B. P.: Isotopic constraints on origins, *Earth Planet. Sci. Lett.*, *111*, 175–182.

Hall, I. R., I. N. McCave, R. Zahn, L. Carter, P. C. Knutz, and G. P. Weedon (2003), Paleocurrent reconstruction of the deep Pacific inflow during the middle Miocene: Reflections of East Antarctic Ice Sheet growth, *Paleoceanography*, *18*(2), 1040, doi:10.1029/2002PA000817.

Henken-Mellies, W. U., J. Beer, F. Heller, K. J. Hsü, C. Shen, G. Bonani, H. J. Hofmann, M. Suter, and W. Wölfli (1990), ^{10}Be and ^{9}Be in South Atlantic DSDP site 519: Relation to geomagnetic reversals and to sediment composition, *Earth Planet. Sci. Lett.*, *98*, 267–276.

Herzer, R. H. (1995), Seismic stratigraphy of a buried volcanic arc, Northland, New Zealand, and implications for Neogene subduction, *Mar. Petrol. Geol.*, *12*, 511–533.

Jeandel, C. (1993), Concentration and isotopic composition of Nd in the South Atlantic Ocean, *Earth Planet. Sci. Lett.*, *117*, 581–591.

Jeandel, C., J. K. Bishop, and A. Zindler (1995), Exchange of neodymium and its isotopes between seawater and small and large particles in the Sargasso Sea, *Geochim. Cosmochim. Acta*, *59*, 535–547.

Johnson, G. C., D. L. Rudnick, and B. A. Taft (1994), Bottom water variability in the Samoa Passage, *J. Mar. Res.*, *52*, 177–196.

Kennett, J. P. (1977), Cenozoic evolution of Antarctic glaciation, the circum-Antarctic Ocean, and their impact on global paleoceanography, *J. Geophy. Res.*, *82*(27), 3843–3860.

Kennett, J. P., and L. D. Stott (1990), Proteus and proto-Oceanus: Ancestral Paleogene oceans as revealed from Antarctic stable isotopic results, *Proc. Ocean Drill. Program Sci. Results*, *113*, 865–880.

Kennett, J. P., and C. C. von der Borch (1986), Southwest Pacific Cenozoic paleoceanography, *Initial Rep. Deep Sea Drill. Proj.*, *90*, 493–1517.

Kennett, J. P., G. Keller, and M. S. Srinivasan (1985), Miocene planktonic foraminiferal biogeography and paleoceanographic development of the Indo-Pacific region, in *The Miocene Ocean: Paleoceanography and Biogeography*, *Geol. Soc. of Am. Mem.*, vol. 163, edited by J. P. Kennett, pp. 197–236, Geol. Soc. of Am., Boulder, Colo.

Larson, R. L., R. A. Pockalny, R. F. Viso, E. Erba, L. J. Abrams, B. P. Luyendyk, J. M. Stock, and R. W. Clayton (2002), Mid-Cretaceous tectonic evolution of the Tongareva triple junction in the southwestern Pacific Basin, *Geology*, *30*, 67–70.

Latimer, J. C., and G. M. Filippelli (2002), Eocene and Miocene terrigenous inputs and export production: Geochemical evidence from ODP Leg 177, Site 1090, *Palaeogeogr. Palaeoclimatol. Palaeoecol.*, *182*, 151–164.

Lawver, L. A., and L. M. Gahagan (1998), Opening of Drake Passage and its impact on Cenozoic ocean circulation, in *Tectonic Boundary Conditions for Climate Reconstructions*, edited by T. J. Crowley and K. C. Burke, pp. 212–223, Oxford Univ. Press, New York.

Lawver, L. A., and L. M. Gahagan (2003), Evolution of Cenozoic seaways in the circum-Antarctic region, *Palaeogeogr. Palaeoclimatol. Palaeoecol.*, *198*, 11–37.

Lear, C. H., H. Elderfield, and P. A. Wilson (2000), Cenozoic deep-sea temperatures and global ice volumes from Mg/Ca in benthic foraminiferal calcite, *Science*, *287*, 269–272.

Lee, T.-Y., and L. A. Lawver (1995), Cenozoic plate reconstruction of southeast Asia, *Tectonophysics*, *251*, 85–138.

Ling, H. F., K. W. Burton, R. K. O'Nions, B. S. Kamber, F. von Blanckenburg, A. J. Gibb, and J. R. Hein (1997), Evolution of Nd and Pb isotopes in central Pacific seawater from ferromanganese crusts, *Earth Planet. Sci. Lett.*, *146*, 1–12.

Linthout, K., H. Helmers, and J. Sopaheluwakan (1997), Late Miocene obduction and microplate migration around the southern Banda Sea and the closure of the Indonesian Seaway, *Tectonophysics*, *281*, 17–30.

Lugmair, G. W., and S. J. G. Galer (1992), Age and isotopic relationships among the angrites Lewis Cliff 86010 and Angra dos Reis, *Geochim. Cosmochim. Acta*, *56*, 1673–1694.

Manheim, F. T. (1986), Marine cobalt resources, *Science*, *232*, 600–608.

McKenzie, J. A., and P. J. Davies (1993), Cenozoic evolution of carbonate platforms on the northeastern Australian margin: Synthesis of Leg 133 drilling sites, *Proc. Ocean Drill. Program Sci. Results*, *133*, 763–770, Ocean Drill. Program, College Station, Tex.

Miller, K. G., R. G. Fairbanks, and G. S. Mountain (1987), Tertiary oxygen isotope synthesis, sea level history, and continental margin erosion, *Paleoceanography*, *2*, 1–19.

Nishimura, S., and S. Suparka (1997), Tectonic approach to the Neogene evolution of Pacific-Indian Ocean seaways, *Tectonophysics*, *281*, 1–16.

Oberhänsli, H. (1992), The influence of the Tethys on the bottom waters of the early Tertiary Ocean, in *The Antarctic Paleoenvironment: A Perspective on Global Change*, *Part One*, edited by J. P. Kennett and D. A. Warnke, pp. 167–184, AGU, Washington, D. C.

Orsi, A. H., G. C. Johnson, and J. L. Bullister (1999), Circulation, mixing, and production of Antarctic Bottom Water, *Progr. Oceanogr.*, *43*, 55–109.

Pfuhl, H. A., I. N. McCave, and S. A. Schellenberg (2002), Changes in Southern Ocean circulation across the Oligocene-Miocene boundary, *Eos Trans. AGU*, *83*(47), Fall Meet. Suppl., Abstract OS21A-0184.

Ramsay, A. T. S., C. W. Smart, and J. C. Zachos (1998), A model of early to middle Miocene deep ocean circulation for the Atlantic and Indian Oceans, *Geol. Soc. Spec. Publ.*, *131*, 55–71.

Reid, J. L. (1997), On the total geostrophic circulation of the pacific ocean: Flow patterns, tracers, and transports, *Progr. Oceanogr.*, *39*, 263–352.

Reid, J. L., and P. F. Lonsdale (1974), On the flow of water through the Samoan Passage, *J. Phys. Oceanogr.*, *4*, 58–73.

Rintoul, S. R., C. W. Hughes, and D. Olbers (2001), The Antarctic Circumpolar Current System, in *Ocean Circulation and Climate—Observing and Modeling the Global Ocean*, edited by G. J. Siedler, J. Church, and J. Gould, pp. 271–302, Academic, San Diego, Calif.

Romine, K., and G. Lombari (1985), Evolution of Pacific circulation in the Miocene: Radiolarian evidence from DSDP Site 289, in *The Miocene Ocean: Paleoceanography and Biogeography*, *Geol. Soc. of Am. Mem.*, vol. 163, edited by J. P. Kennett, pp. 273–290, Geol. Soc. of Am., Boulder, Colo.

Rudnick, D. L. (1997), Direct velocity measurements in the Samoan Passage, *J. Geophys. Res.*, *102*(C2), 3293–3302.

Schaule, B. K., and C. C. Patterson (1981), Lead concentrations in the northeast Pacific: Evidence for global anthropogenic perturbations, *Earth Planet. Sci. Lett.*, *54*, 97–116.

Scher, H., and E. E. Martin (2003), Eocene to Miocene Southern Ocean circulation: Neodymium records from fossil fish teeth, *Geophys. Res. Abstr.*, *5*, 06643.

Schmitz, W. J., Jr. (1995), On the interbasin-scale thermohaline circulation, *Rev. Geophys.*, *33*, 151–173.

Schmitz, W. J., Jr. (1996), *On the World Ocean Circulation*, vol. II, *The Pacific and Indian Oceans–A Global Update*, *Tech. Rep.WHOI-96-08*, Woods Hole Oceanogr. Inst., Woods Hole, Mass.

Sclater, J. G., L. Meinke, A. Bennett, and C. Murphy (1985), The depth of the ocean through the Neogene, in *The Miocene Ocean: Paleoceanography and Biogeography*, *Geol. Soc. of Am. Mem.*, vol. 163, edited by J. P. Kennett, pp. 1–19, Geol. Soc. of Am., Boulder, Colo.

Shackleton, N. J., and J. P. Kennett (1975), Paleotemperature history of the Cenozoic and the initiation of Antarctic glaciation: Oxygen and carbon isotope analyses in DSDP sites 277, 279, and 281, *Initial Rep. Deep Sea Drill. Proj.*, *29*, 143–156.

Sokolov, S., and S. Rintoul (2000), Circulation and water masses of the southwest Pacific: WOCE Section P11, Papua New Guinea to Tasmania, *J. Mar. Res.*, *58*, 223–268.

Spero, H. J., J. Bijma, D. W. Lea, and B. E. Bemis (1997), Effect of seawater carbonate concentration on foraminiferal carbon and oxygen isotopes, *Nature*, *390*, 497–500.

Tachikawa, K., and C. Jeandel (1999), A new approach to the Nd residence time in the ocean: The role of atmospheric inputs, *Earth Planet. Sci. Lett.*, *170*, 433–446.

Taft, B. A., S. P. Hayes, G. E. Friederich, and L. A. Codispoti (1991), Flow of abyssal water into the Samoa Passage, *Deep Sea Res.*, *38*, S103–S128.

Tsuchi, R. (1997), Marine climatic responses to Neogene tectonics of the Pacific Ocean seaways, *Tectonophysics*, *281*, 113–124.

Ulfbeck, D. G., J. A. Baker, I. J. Graham, and I. C. Wright (2001), Hf isotopic profiles of Fe-Mn nodules (19-0 Ma) from the deep western boundary current, southern Pacific, *Eos Trans. AGU*, *82*(47), Fall Meet. Suppl., Abstract OS31C-0439.

van de Flierdt, T., M. Frank, A. N. Halliday, J. R. Hein, B. Hattendorf, D. Günther, and P. W. Kubik (2003), Lead isotopes in North Pacific Deep Water—Implications for past changes in input sources and circulation patterns, *Earth Planet. Sci. Lett.*, *209*, 149–164.

Vlastélic, I., W. Abouchami, S. J. G. Galer, and A. W. Hofmann (2001), Geographic control on Pb isotope distribution and sources in Indian Ocean Fe-Mn deposits, *Geochim. Cosmochim. Acta*, *65*(23), 4303–4319.

von Blanckenburg, F., and H. Igel (1999), Lateral mixing and advection of reactive isotope tracers in ocean basins: Observations and mechanisms, *Earth Planet. Sci. Lett.*, *169*, 113–128.

von Blanckenburg, F., R. K. O'Nions, N. S. Belshaw, A. Gibb, and J. R. Hein (1996a), Global distribution of beryllium isotopes in deep ocean water as derived from Fe-Mn crusts, *Earth Planet. Sci. Lett.*, *141*, 213–226.

von Blanckenburg, F., R. K. O'Nions, and J. R. Hein (1996b), Distribution and sources of pre-

anthropogenic lead isotopes in deep ocean water from Fe-Mn crusts, *Geochim. Cosmochim. Acta*, *60*(24), 4957–4963.

Walder, A. J., I. Platzner, and P. A. Freedman (1993), Isotope ratios measurement of lead, neodymium and neodymium-samarium mixtures, hafnium and hafnium-lutetium mixtures with a double focussing multiple collector inductively coupled plasma mass spectrometer, *J. Anal. Atom. Spectrom.*, *8*, 19–23.

Wei, K.-Y. (1998), Southward shifting of the Tasman Front at 4.4 Ma (early Pliocene): Paleobiogeographic and oxygen isotopic evidence, *J. Asian Earth Sci.*, *16*, 97–106.

Wijffels, S. E., J. M. Toole, and R. Davis (2001), Revisiting the South Pacific subtropical circulation: A synthesis of World Ocean Circulation Experiment observations along 32°S, *J. Geophys. Res.*, *106*(C9), 19,481–19,513.

Woodruff, F., and S. M. Savin (1989), Miocene deepwater oceanography, *Paleoceanography*, *4*, 87–140.

Wright, J. D., and K. G. Miller (1993), Southern Ocean influences on Late Eocene to Miocene deepwater circulation, in *The Antarctic Paleoenvironment: A Perspective on Global Change*, *Part Two*, edited by J. P. Kennett and D. A. Warnke, pp. 1–25, AGU, Washington, D. C.

Wright, J. D., K. G. Miller, and R. G. Fairbanks (1992), Early and middle Miocene stable isotopes: Implications for deepwater circulation and climate, *Paleoceanography*, *7*, 357–389.

Wyrtki, K. (1960), *The Surface Circulation in the Coral and Tasman Seas*, 44 pp., *Div. Fish. Oceanogr. Tech. Pap. 8*, Commonw. Sci. and Ind. Res. Org., Melbourne, Vict., Australia.

Zachos, J., M. Pagani, L. Sloan, E. Thomas, and K. Billups (2001), Trends, rhythms, and aberrations in global climate 65 Ma to present, *Science*, *292*, 686–693.

M. Frank and A. N. Halliday, Institute for Isotope Geology and Mineral Resources, Department of Earth Sciences, ETH-Zentrum, Sonneggstrasse 5, CH-8092 Zürich, Switzerland.

D. Günther and B. Hattendorf, Laboratory of Inorganic Chemistry, Department of Chemistry, ETH Hönggerberg, Wolfgang-Pauli-Strasse 10, CH-8093 Zürich, Switzerland.

J. R. Hein, U.S. Geological Survey, 345 Middlefield Road, MS-999, Menlo Park, CA 94025, USA.

P. W. Kubik, Paul Scherrer Institute, c/o Institute for Particle Physics, ETH Hönggerberg, CH-8093 Zürich, Switzerland.

T. van de Flierdt, Lamont-Doherty Earth Observatory, Columbia University, 61 Route 9W, Palisades, NY 10964, USA. (tina@ldeo.columbia.edu)